Biosensors and Bioelectronics ■ (■■■■) ■■■–■■■

Contents lists available at ScienceDirect

Biosensors and Bioelectronics

journal homepage: www.elsevier.com/locate/bios

An electrochemical sensor for detection of neurotransmitter-acetylcholine using metal nanoparticles, 2D material and conducting polymer modified electrode

Nidhi Chauhan [a], Sheetal Chawla [b], C.S. Pundir [c], Utkarsh Jain [a,*]

[a] Amity Institute of Nanotechnology, Amity University, Noida 201303, Uttar Pradesh, India
[b] Disease Biology Laboratory, Regional Centre for Biotechnology, National Capital Region Biotech Science Cluster, Faridabad, Haryana, India
[c] Department of Biochemistry, M.D. University, Rohtak 124001, Haryana, India

ARTICLE INFO

Article history:
Received 26 May 2016
Received in revised form
13 June 2016
Accepted 14 June 2016

Keywords:
Choline oxidase
Acetylcholinesterase
Iron oxide nanoparticles, graphene oxide, poly(3,4-ethylenedioxythiophene)

ABSTRACT

An essential biological sensor for acetylcholine (ACh) detection is constructed by immobilizing enzymes, acetylcholinesterase (AChE) and choline oxidase (ChO), on the surface of iron oxide nanoparticles (Fe_2O_3NPs), poly(3,4-ethylenedioxythiophene) (PEDOT)-reduced graphene oxide (rGO) nanocomposite modified fluorine doped tin oxide (FTO). The qualitative and quantitative measurements of nanocomposites properties were accomplished by scanning electron microscope (SEM), electrochemical impedance spectroscopy (EIS) and cyclic voltammetry (CV). This prepared biological sensor delineated a wide linear range of 4.0 nM to 800 μM with a response time less than 4 s and detection limit (based on S/N ratio) of 4.0 nM. The sensor showed perfect sensitivity, excessive selectivity and stability for longer period of time during storage. Besides its very high-sensitivity, the biosensor has displayed a low detection limit which is reported for the first time in comparison to previously reported ACh sensors. By fabricating Fe_2O_3NPs/rGO/PEDOT modified FTO electrode for determining ACh level in serum samples, the applicability of biosensor has increased immensely as the detection of the level neurotransmitter is first priority for patients suffering from memory loss or Alzheimer's disease (AD).

1. Introduction

Acetylcholine (ACh), an organic chemical, is released by nerve cells to deliver signals to the other cell types and acts as a neurotransmitter. It was first discovered in central nervous system (Francis et al., 1999). ACh and its metabolite choline (Ch) play vital roles in brain chemistry (Çevik et al., 2012). They are needed for three main physiological functions i.e. learning, memory and attention. Inside the nervous system, ACh functions as neuromodulator in both peripheral nervous system (PNS) and central nervous system (CNS). Since loss of neuro-transmission and -modulation are linked with ACh, the several neural disorders are therefore associated with ACh including Alzheimer's disease (AD), Parkinson diseases, schizophrenia and progressive dementia. According to the cholinergic hypothesis, Alzheimer's disease is occurred due to reduced synthesis of the ACh (Rizzo et al., 2008). In order to understand the functional and physiological aspects of neural disorders caused by decrease in ACh concentration and their cure, a sensitive, rapid and accurate detection tool is utmost required in clinical applications (Yang et al., 2005; Xue et al., 2008; Shimomura et al., 2009; Lopez et al., 2007).

The detection of ACh and Ch are based on the following enzyme reactions:

$$\text{Acetylcholine} + H_2O \xrightarrow{\text{AChE}} \text{Choline} + \text{Acetate}$$

$$\text{Choline} + O_2 \xrightarrow{\text{ChO}} \text{Betaine aldehyde} + H_2O_2$$

During electrochemical biological sensing, Ch is formed by enzymatic reaction using the enzyme AChE after interacting the substrate ACh. The current generated by the oxidation of hydrogen peroxide is linearly related to Ch and the oxidation current is in turn proportional to the substrate ACh concentration used in the reaction.

In order to increase the sensitivity of biosensor and further facilitate an electron transfer, an important factor i.e. conductivity for working electrodes must be taken into consideration (Dutta et al., 2016; Chauhan et al., 2015). Therefore present researches which are carried out to modify working electrode surfaces with nanomaterials for instance graphene, carbon nanotubes and gold nanoparticles, are focussing on increasing surface to volume ratio and conductivity (Pundir et al., 2011). The exceptional

* Corresponding author.
E-mail address: utkarshmicromvp@gmail.com (U. Jain).

http://dx.doi.org/10.1016/j.bios.2016.06.047
0956-5663/

electrochemical conductance of graphene indicates that it is a commendable electrode material in electroanalysis (Shao et al., 2010). Graphene oxide (GO) which contains oxygen functional groups and have edges, is normally a single sheet of GO and shows an excellent conducting behaviour (Wang et al., 2010). The solubility in the water and in other solvents permit GO into uniform deposition on the wide range of substrates of thin films and networks. These characteristics make it potentially useful for macroelectronics (Mkhoyan et al., 2009). The discrete GO sheet has a flat surface which may serve as an ideal solid substrate atomically for enzyme immobilization (Zhang et al., 2010). Following their electrochemical behaviours and significant conducting properties, GO nanomaterials are increasingly well studied for enzyme immobilization and biosensor applications (Liu et al., 2010).

In biological sensing applications, the poly(3,4-ethylenedioxythiophene) (PEDOT) is used as a modifier for electrode. PEDOT is used in conducting polymers. PEDOT is very stable, eco-friendly, imparts a fast electron transfer and used in easy formation of strong-willed films (Jun et al., 2010). In addition, by using PEDOT to modify the electrode forming PEDOT-rGO modified electrode has shown significant electrocatalytic effect for different sensor applications (Yajie et al., 2014; Xiaoliang et al., 2014; Wang et al., 2014). The modified electrode using PEDOT forms a base for metal-oxide enzyme and PEDOT/GO nanocomposite which combines the excellent properties of both, conducting polymer and GO. Their combination is promising for many applications. Considering these properties, we expect that the loading of Fe_3O_4 nanoparticles on composite material will provide a unique and consecutive combination for the electrocatalytic oxidation of ACh. In this work, we have prepared the nanocomposite/sensing interface by using metal nanoparticles with combination of graphene-PEDOT (PEDOT is a conducting polymer). Sriprachuabwong et al. (2012) described graphene-PEDOT (GR-PEDOT) modified electrode by showing a high efficiency in electrochemical sensing which were used in our study. We have used metallic nanoparticles (Fe_2O_3), a conductive polymer (PEDOT) and carbon-based nanomaterial (rGO). In order to enhance the electrical conductivity, the combination of rGO with materials including polymer and metal were used.

In our work, we employed Fe_2O_3/PEDOT-rGO composite on fluorine doped tin oxide (FTO) surface for sensing ACh. The electrochemical sensing methods including cyclic voltammerty and electrochemical impedance spectroscopy (EIS) technique were incorporated for fast and relatively sensitive detection and characterization. The nanocomposites in our study were used for the first time and has not been reported previously. This implies an ultrasensitive detection of ACh. The nanocomposites act as a sensing matrix for amperometric detection of ACh after necessary pre-treatment. Comparing with the other electrochemical methods, the newly developed sensor was effectively used for determining ACh concentration and revealed an elevated sensitivity, lesser detection limit and a faster implementation. The linear range of the biological sensor for detecting ACh in the sample is 4.0 nM to 800 μM.

2. Experimental

2.1. Chemicals and reagents

AChE (EC 3.1.1.7, type VI-S; from electric eel; activity 200–600 U/mg solid), ChO (EC 1.1.3.17, from *Alcaligenes*, sp. 10 U/mg solid), fluorine-doped tinoxide (FTO) glass electrode (100 mm × 100 mm × 2.3 mm) with usual resistance of approximately ~7 Ω/Sq, 3,4-Ethylenedioxythiophene (EDOT, 98%), glutaraldehyde and acetylcholine chloride (AChCl) were bought from Sigma Chemical Co. USA. $FeCl_2$. Sodium fluoride and ammonium hydroxide were purchased from Sisco Research Laboratory, Mumbai. The chemicals used in the experiments were completely analytical reagent grade. In all the experiments only double distilled water (DW) was used. The buffers used in experiments were oxygen saturated. Electrochemical measurements were conducted with a potentiostat/galvanostat (model: Autolab AUT83785, Ecochemie, The Netherlands).

2.2. Preparation of graphene oxide nanosheet (GONS)

Hummers and Offeman (1958) suggested a modified method for preparation of GONS. Firstly, at 4 °C, 0.5 g of graphite powder was dissolved in 23 mL of H_2SO_4 and then 0.5 g of $NaNO_3$ was added. Thereafter, 10 mL of $KMnO_4$ (2 mM) was mixed drop by drop and the slurry was further stirred in water bath for 1 h at 35°C. DDW (140 mL) was further mixed and boiled at 90 °C. In the last, 3 mL of H_2O_2 (30 wt%) was added and mixed until a light brown color was appeared. Finally, GONS was collected by washing, filtering and then centrifugation at 4000 rpm.

2.3. Preparation of enzymes/Fe_2O_3/rGO-PEDOT modified electrode

Firstly, the FTO electrode was thoroughly cleaned with acetone using ultrasonic bath for 10 min and later with DW for further 10 min. After doping GO by PEDOT film, an electropolymerisation method was used to deposit GO-PEDOT film on the FTO electrode while potential cycling was taken in the range of −0.2 to 1.2 V vs. Ag/AgCl with scan rate 50 mV s^{-1}. Solution containing 10 mM of EDOT and 1 mg mL^{-1} of GO were mixed for doping. An amperometric method, suggested by Wang et al. (2014), was applied for electrochemical reduction of PEDOT-GO at −0.9 V for 600 s at pH 7.4. Synthesis of Fe_2O_3 was performed by hydrothermal method. In short, $FeCl_2$ (0.1 g), sodium fluoride (0.05 g) and ammonium hydroxide (0.01 g) were mixed together and further stirred at magnetic stirrer for 15 min and then transferred into the 30 mL telfon sealed autoclave (Dong et al., 2012; Ming et al., 2014). After mixing, solution was heated at 170 °C for 12 h and then cooled at room temperature. A precipitate was formed which was further washed with ethanol and deionised (DI) water 3:1. Finally, α-Fe_2O_3 was dried at 90 °C for 24 h. 1 mg of α-Fe_2O_3, 2 mg mL^{-1} of AChE and ChOx enzyme in phosphate buffer (pH 7.0) was prepared. 2.5 wt% of glutaraldehyde as cross linking agent were mixed in 10 mL of the prepared enzyme and mixed well for 15 min by applying 60 rpm at 0 °C for 2 V.

2.4. Entrapment of enzyme

10 mL of the enzyme mixture was prepared and drop wise added to the PEDOT/rGO modified FTO electrode and then allowed to air dried at 4 °C. The unbound cross linked enzyme on the surface of the prepared AChE-ChO/Fe_2O_3/rGO/PEDOT/FTO electrode was removed by applying washing buffer to the surface of electrode (Scheme 1).

2.5. Characterization by electrochemical measurement

Characterization of AChE-ChO/Fe_2O_3/rGO/PEDOT/FTO electrode was performed through electrochemical measurements. The process of analysis is carried out by a three-electrode system where the AChE-ChO/Fe_2O_3/rGO/PEDOT/FTO coated glass plate acts as a working electrode. The auxiliary electrode is a Pt wire and the reference electrode is an Ag/AgCl (saturated 3 M KCl) electrode. Firstly before the analysis, the pre-equilibration of the electrode system was accomplished at +0.2 V for the period 15 s and each time during detection. The steady current readings were taken at +0.2 V (vs. Ag/AgCl). AChCl (100 μL, 0.05 M) solution was applied

Please cite this article as: Chauhan, N., et al., Biosensors and Bioelectronics (2016), http://dx.doi.org/10.1016/j.bios.2016.06.047

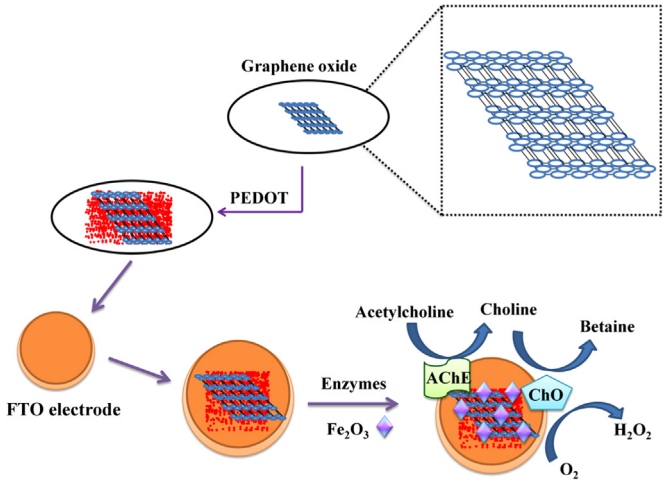

Scheme 1. Schematic illustration of the AChE-ChO/Fe_2O_3/rGO/PEDOT nanocomposite onto the FTO-coated glass plate and subsequent recognition of ACh.

to the cell containing 20 mL electrolyte [2.5 mM $K_3Fe(CN)_6/K_4Fe(CN)_6$ (1:1)]. Furthermore, +0.2 V of voltage was applied. These electroanalytical analyses were performed at room temperature.

2.6. Optimization of electrode

AChE-ChO/Fe_2O_3/rGO/PEDOT/FTO coated glass plate electrode was optimized for ACh measurements. The optimization was achieved by two different buffers testing at various pH range; Phosphate buffer (pH 5.5–7.5) and Borate buffer (pH 8.0–10.0) (each at 0.1 M). Both buffers are mixed with 0.1 M potassium chloride. In order to determine optimum temperature of the reaction mixture, the range of 20–55 °C (intervals of 5 °C) temperatures were analyzed. The substrate concentration was tested by cyclic voltammetry using various AChCl concentrations which were ranging from 0.002 to 800 μM. The responses of interfering species including glucose, ascorbic acid, urea, 4-acetamidophenol, bilirubin and uric acid having concentration of 0.1 mM were analyzed amperometrically .

2.7. Stability and reproducibility of the biosensor

A washing step was performed by dipping the working electrode in 5 mL of 0.1 M phosphate buffer at pH 7.0. The washing step is performed for further use of working electrode. The storage stability of the biosensor was further checked over the period of 4-months. The AChE-ChO/Fe_2O_3/rGO/PEDOT/FTO coated glass plate was always kept dry in a refrigerator at 4 °C temperature. The activity was evaluated once in a week.

3. Results and discussion

3.1. SEM study of modified electrode

The change in morphology at the surface of FTO coated glass plate is depicted in Fig. 1. The study of this change was carried out by SEM in chronological order firstly after modification by deposition of Fe_2O_3/rGO/PEDOT/FTO and then immobilization of AChE-ChO. A uniform and smooth surface is shown by bare FTO coated glass plate (a) whereas layer of rGO/PEDOT on FTO coated glass plate demonstrated formation of almost uniform surface (b). The SEM image of the Fe_2O_3/rGO/PEDOT/FTO also exhibits the dots of Fe_2O_3 (c). The SEM of AChE-ChO/Fe_2O_3/rGO/PEDOT/FTO coated glass plate (d) demonstrates an immobilization of the enzyme having regular globular structural morphology on the surface of modified electrode indicating the formation of their sensing matrix.

3.2. Electrochemical impedance measurements

Fig. 2(a) depicts an electrochemical impedance spectra (EIS) of bare FTO-coated glass plate (a), rGO/PEDOT/FTO (b), Fe_2O_3/rGO/PEDOT/FTO coated glass plate (c) and AChE-ChO/Fe_2O_3/rGO/PEDOT nanocomposite on the FTO coated glass plate (d) in 5.0 mM $K_3Fe(CN)_6/K_4Fe(CN)_6$ (1:1) with polarization potential of 0.20 mV s^{-1} in the frequency range of 0.01 Hz–12 kHz.

rGO/PEDOT nanostructure modified sensing electrode shows smaller charge transfer resistance (R_{CT}) 4500 Ω, when compared with bare FTO electrode which shows almost linear spectrum (6000 Ω). Nyquist plot of Fe_2O_3/rGO/PEDOT/FTO coated glass plate (curve b) showed an R_{CT} value of 4000 Ω indicating a superior conductance of electrons in the Fe_2O_3 modified rGO/PEDOT. Also, an electron transfer between the electrode and the redox probe was competent. The semicircle diameter was enlarged after immobilization of AChE-ChO on Fe_2O_3/rGO/PEDOT/FTO coated glass plate as compared to nanocomposite modified electrode resulting in an increased R_{CT} value of 5000 Ω. Since most biological molecules including enzymes are poor electrical conductors at low frequencies (at least <10 kHz), the increase in R_{CT} is attributed to the fact that these molecules cause obstacles in transfer of electrons.

3.3. Cyclic voltammerty study

Cyclic voltammetry studies were performed for evaluation of charge-transfer properties occurred on the surface of electrodes after modification. Potassium ferricyanide-potassium ferrocyanide solution was used as electrolyte.

The cyclic voltammograms recorded for (a) rGO/FTO electrode, (b) rGO/PEDOT/FTO electrode and (c) Fe_2O_3/rGO/PEDOT/FTO electrode. When the electrode was modified by rGO/PEDOT, a very clear oxidation peak was observed (Supplementary Fig. 1). The electrodeposition of rGO/PEDOT on FTO electrode surface led to the vast increase in current intensity as a result of the increase in electro active area. CV of Fe_2O_3/rGO/PEDOT/FTO electrode in curve c showed greatly an enhanced current with well defined oxidation and reduction peaks. This is credited solely to the presence of rGO with another materials: polymer and metal, which were used to enhance the electrical conductivity and larger specific surface area. The obtained values on rGO/FTO, rGO/PEDOT/FTO and Fe_2O_3/rGO/PEDOT/FTO electrodes were 30, 75 and 90 μA, respectively. This shows the higher current due to the synergetic effect of metallic nanoparticles (Fe_2O_3), conductive polymer (PEDOT) and carbon-based nanomaterial (rGO).

Cyclic voltamogramms (Fig. 3(A)) were operated in 2.5 mM $K_3Fe(CN)_6/K_4Fe(CN)_6$ [(1:1)] and 0.1 M phosphate buffer (pH 7.0). After recording CV, bare FTO coated glass plate did not show any peak (curve a). The cyclic voltammogram of Fe_2O_3/rGO/PEDOT/FTO coated glass plate identified an oxidation peak at 0.25 V (vs. Ag/AgCl) (curve b). The electrodeposition of Fe_2O_3/rGO/PEDOT onto FTO coated glass plate surface may lead to elevation in intensity of the current. Furthermore, the immobilizations of AChE and ChO were performed on the nanocomposites. Once immobilization is completed, the cyclic voltammogram was carried out as shown in trace c. An increase from 75 (trace c) to 120 μA (trace c) peak current ratio between reduction to oxidation was obtained which indicates that AChCl biosensing has improvement in its reversible direct electron transfer property.

Please cite this article as: Chauhan, N., et al., Biosensors and Bioelectronics (2016), http://dx.doi.org/10.1016/j.bios.2016.06.047

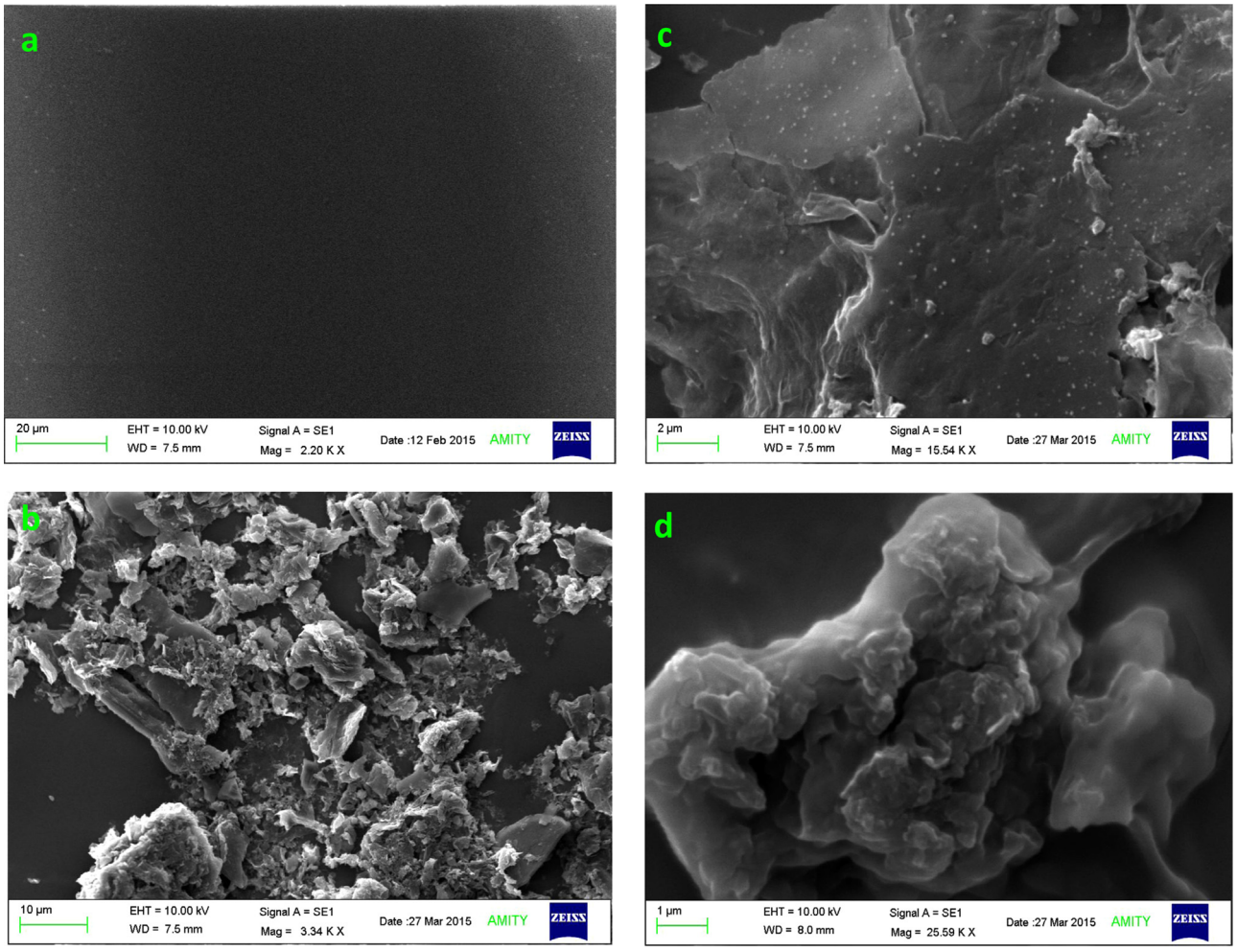

Fig. 1. SEM images of (a) bare FTO coated glass plate, (b) rGO/PEDOT/FTO coated glass plate, (c) Fe_2O_3/rGO/PEDOT/FTO coated glass plate and (d) AChE-ChO/Fe_2O_3/rGO/PEDOT nanocomposite onto the FTO coated glass plate.

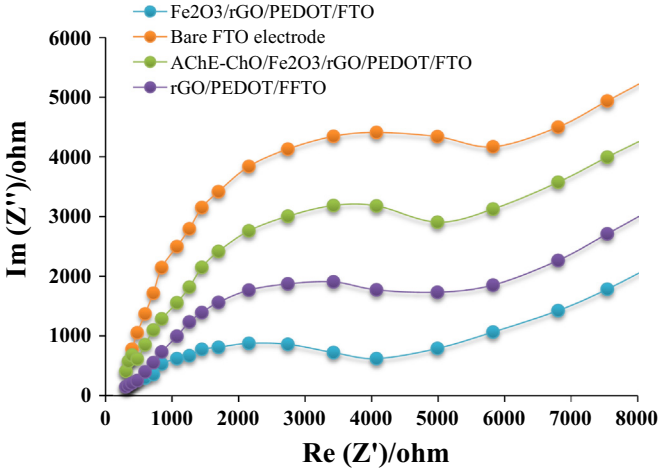

Fig. 2. EIS behaviour of the bare FTO-coated glass plate (a), rGO/PEDOT/FTO (b), Fe_2O_3/rGO/PEDOT/FTO coated glass plate (c) and AChE-ChO/Fe_2O_3/rGO/PEDOT/FTO coated glass plate (d). The electrolyte consists of 5.0 mM $K_3[Fe(CN)_6]$ and 0.1 M KCl at 0.20 mV s^{-1} in sodium phosphate buffer. (Frequency range of 0.01 Hz–10 kHz).

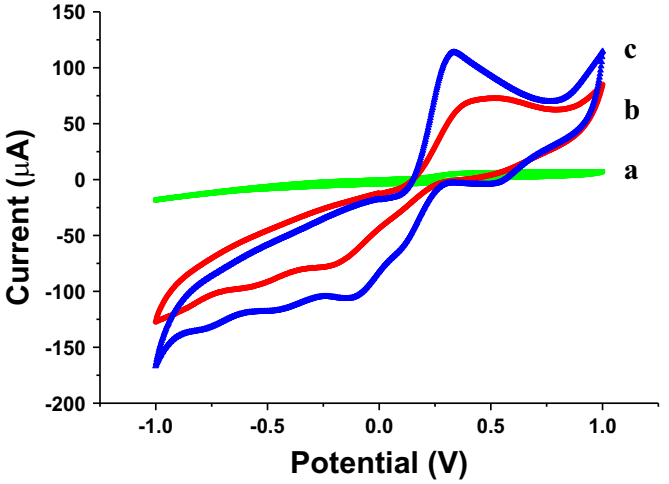

Fig. 3. Cyclic voltammograms of bare FTO-coated glass plate (a), Fe_2O_3/rGO/PEDOT/FTO coated glass plate (b) and AChE-ChO/Fe_2O_3/rGO/PEDOT/FTO coated glass plate (c).

3.4. Optimizing biosensor prototype for test conditions

AChE-ChO/Fe_2O_3/rGO/PEDOT/FTO coated glass plate was evaluated by cyclic voltammetry. The potential range in 1.0 mL of 0.1 mM AChCl with 14 mL of 0.1 M phosphate buffer (pH 7.0) was shown as −1.0 to +1.0 V against Ag/AgCl as reference electrode while the scan rate was recorded as 20 mV s^{-1}. At +0.2 V of potential difference the response was optimum therefore +0.2 V of voltage was taken in all the experiments. The optimum response

Please cite this article as: Chauhan, N., et al., Biosensors and Bioelectronics (2016), http://dx.doi.org/10.1016/j.bios.2016.06.047

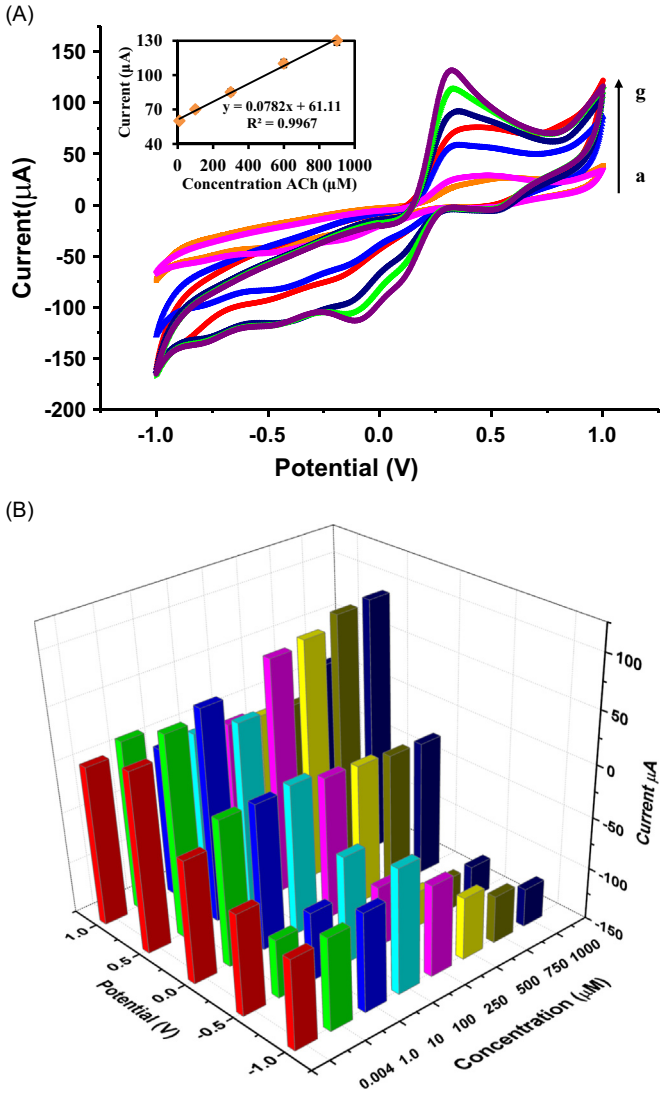

Fig. 4. (A) Cyclic voltammograms recorded at different concentrations of AChCl from 0.004 μM (a), 1.0 μM (b), 10 μM (c), 200 μM (d), 400 μM (e), 600 μM (f) and 800 μM (g). Scan rate: 50 mV s^{-1} [Inset: Calibration curve for ACh biosensor]. (B) 3D image of different concentration of substrate i.e. AChCl.

of the biosensor was exhibited at pH 7.0. The free enzyme has pH of 8.0 which is slightly higher than the optimized pH (Sen et al., 2004). At 30 ºC, the response of AChE-ChO/Fe_2O_3/rGO/PEDOT/FTO coated glass plate was optimum showing similarity in response with free enzyme (30 °C) (Sen et al., 2004) and with previously reported biosensors (30 °C) (Chauhan and Pundir, 2014; Romllon et al., 1992). In the slight change of the pH, these changes occurred physiologically indicating the kinetic properties of the enzymes when immobilization may lead to change in confirmation of many enzymes.

Therefore, all the experiments were conducted at pH 7.0 and 30 °C. The prepared biological sensor showed an optimum response in 4 s.

3.5. Analysis of ACh biological sensor

A cyclic voltammetry plot in the Fig. 4(A) was taken for desired concentrations of AChCl. Each desired concentrations upto 800 μM of AChCl were measured for voltammetry. No significant current was elevated after 800 μM of AChCl concentration. A saturation level of electrode was reached at 800 μM. A steady state response of 95% was attained in 4 s indicating diffusion occurred was very fast.

A relationship obtained between AChCl concentration (in the range of 4.0 nM to 800 μM) and current (μA) was linear (inset of Fig. 4(A)). The stability of the prepared sensor can be judged by the fact that there is no change in the potential at different concentrations of ACh. No shift in potential is observed after visualizing the captivating 3D image (Fig. 4(B)) showing high stability of our sensor. No change in potential at different concentrations of ACh on this fabricated sensor was noticed. As indicated in the Fig. 4 (B), a low current is obtained after evaluating varying concentrations of solution at relatively negative potentials however a high current is observed at positive potentials. Highest response was recorded at concentration of 800 μM. This curve shows a relationship between the response current and ACh concentration for the prepared sensor. As clearly seen in the graph, when concentration of substrate (ACh) increases consequently the response current also increases.

Km for ACh was reported as 25 μM. Lower Km, which indicates an increased affinity of the enzyme toward substrate (ACh) after immobilization, is due to enhanced diffusion of ACh through Fe_2O_3/rGO/PEDOT/FTO coated glass plate. The detection limit and sensitivity of the prepared biological sensor were 4.0 nM (S/N = 3) and 0.39 μA/μM respectively, which is relatively different than that of enzyme electrodes formed by multiwalled carbon nanotubes/zirconium oxide electrodeposited on modified glassy carbon (GC) electrode (Pundir et al., 2012), chitosan/gold-coated ferric oxide nanoparticles modified Au electrode (Chauhan and Pundir, 2014), Au nanorods and polyvinyl alcohol (PVA) modified Pt electrode (Ren et al., 2009), single walled carbon nanotubes on GC electrode (Sajjadi et al., 2011) and phenyl carboxylic acid-grafted multiwalled carbon nanotube modified screen printed electrode (Lee et al., 2014). The mean analytic recoveries of mixed AChCl at 5.0 and 10.0 μM (final concentration in serum) (spiked samples) by the prepared biological sensor were 95.7 ± 0.2 and 97.6 ± 0.3%. In order to check if the prepared biosensor can be used multiple times and is authenticated, an evaluation for ACh content was carried out in six different serum samples (real samples) on a single day (within batch) for five multiple times. The process was further performed once after keeping the sensor at 4 °C for the period of 1 week (between batch). The obtained results were consistent. The coefficients of variation (CVs) were calculated, i.e., 3.15% (within) and 4.65% (between). The results clearly shows that the prepared sensor can be used repeatedly and consistently and have remarkable stability. With this proposed biosensor, it was observed that the immobilization of AChE-ChO onto Fe_2O_3/rGO/PEDOT/FTO coated glass plate was being credited as a crucial component in sensing system.

The values obtained after ACh measurements using our process were further correlated with the standard and widely used commercial method i.e., High Performance Liquid Chromatography (HPLC) having a fair coefficient of regression (R^2 = 0.998) (Fig. 5 (A)). The interferences caused by 4-acetamidophenol, uric acid and ascorbic acid were negligible while measuring ACh by this biosensor. Each interferants were perceived at 0.1 mM concentration. The obtained value in the presence of above interferants for I_{max} was significantly equivalent which indicates no hindrance caused by any interferants (Fig. 5(B)). The acetylcholine biosensors which were prepared previously had showed reduced activity caused by ascorbic acid (Sen et al., 2004; Guerrieri et al., 2006).

3.6. Estimation of ACh in serum samples

ACh concentrations in the serum of healthy volunteers (n = 10) were obtained between 8.2 and 11.3;nM (having mean value 9.26 nM) after measuring with prepared biosensor. This is a normal established level in the healthy persons (i.e. 8.66 ± 1.02 nM) (Lin et al., 2004) and 5.0–7.8 nM having mean value of 6.93 nM in

Please cite this article as: Chauhan, N., et al., Biosensors and Bioelectronics (2016), http://dx.doi.org/10.1016/j.bios.2016.06.047

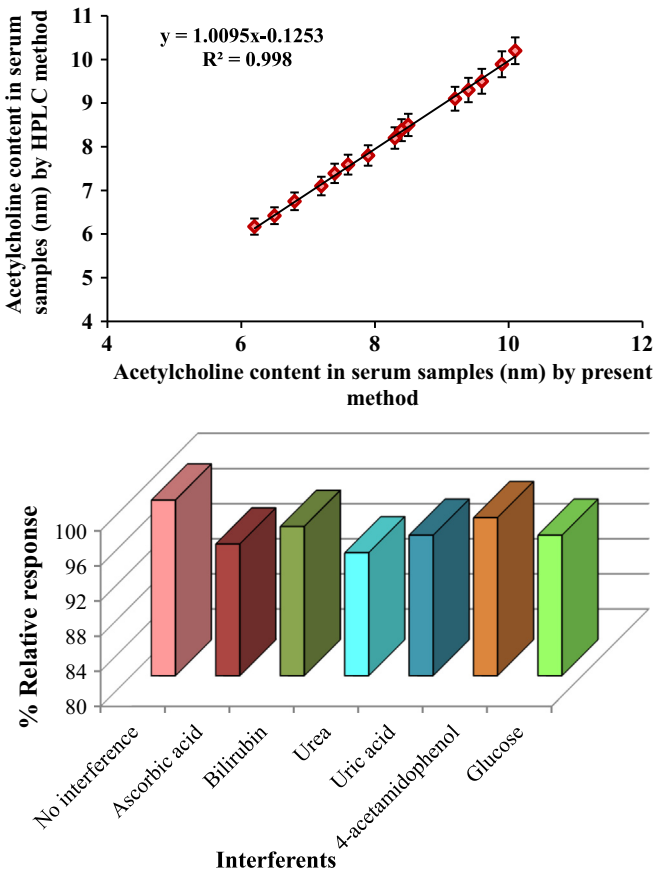

Fig. 5. A. Correlations between ACh values determined by standard HPLC method (y-axis) and current AChE-ChO/Fe_2O_3/rGO/PEDOT modified FTO electrode (x-axis). B. Interference study of different metabolites (each at 0.1 mM) on the activity of AChE-ChO/Fe_2O_3/rGO/PEDOT/FTO coated glass plate. Eap = +0.2 V vs. Ag/AgCl, phosphate buffer pH 7.0 and AChCl concentration 0.5 mM.

patients suffering from Alzheimer's disease (n = 10) (Supplementary Table 1). In our experiments with Alzheimer's patients, a slightly lower but significant ($p < 0.01$) measurements compared to healthy volunteers were noticed. In earlier reports, the amount of ACh is much lower in patients suffering from Alzheimer's disease.

3.7. *Stability and further usability of biological sensor*

The stability for the longer period of time during storage condition of the modified electrode was evaluated by keeping the electrode at room temperature and by examines the response upon certain time periods. The modified electrode was amperometrically significant with no change for first 60 days. After 100 days, only 90% of its original response of the electrodes to AChCl was retained. In order to investigate reproducibility of the prepared biological sensor, five parallel biosensors were compared. The detection of 5.0 mM AChCl was significant with the relative standard deviation of 4.3% which indicates a sufficient performance of the newly developed biosensor.

The analytical properties of all previously reported amperometric ACh biosensors were compared with the present biosensor and therefore revealed an elevated linear range, lesser detection limit and a faster implementation (Supplementary Table 2).

4. Conclusions

In our research work, a successful fabrication of Fe_2O_3/rGO/PEDOT film modified FTO electrode was performed. The synthesized Fe_2O_3/rGO/PEDOT/FTO nanostructures were further analyzed for their structural properties in detail via quantitative and qualitative measurements showing synthesized particle size nanostructures in the range of nm. The constructed sensor was evaluated for desired purpose and many remarkable analytical features were noticed including a wide linear range, fair analytical recovery, multiple reusability, significant selectivity and fast response. Furthermore, Fe_2O_3/rGO/PEDOT nanostructures are firmly harboured on FTO and remain active in long-term (for the period of 100 days). Our work unfolds a method for making use of a sensing interface considering Fe_2O_3/rGO/PEDOT/FTO as a best material for stable and a high potential redox transition using Biosensor Technology suggesting a general approach for robust, consistent detection in biological systems.

This ACh biosensor, when integrated with associated signal conditioning and processing circuits, promises high sensitivity and cheaper manufacturing costs than other enzyme sensing systems. By using these nanocomposites (Fe_2O_3/rGO/PEDOT) and their multiple usability (good stability and repeatability) will definitely reduce the cost of the product over the long term then present a robust commercial enzyme sensing system.

Acknowledgement

Dr. Utkarsh Jain & Dr. Nidhi Chauhan received “Start up Research Grants” by Science and Engineering Research Board (SERB), Department of Science & Technology (DST), Government of India. The SERB-DST is greatly acknowledged.

Appendix A. Supplementary material

Supplementary data associated with this article can be found in the online version at http://dx.doi.org/10.1016/j.bios.2016.06.047.

References

Çevik, S., Timur, S., Anik, Ü., 2012. Microchim. Acta 179, 299–305.
Chauhan, N., Pundir, C.S., 2014. Biosens. Bioelectron. 61, 1–8.
Chauhan, N., Narang, J., Jain, U., 2015. Analyst 140, 1988–1994.
Dong, Q., Yin, S., Guo, C.S., Li, H.H., Kumada, N., Takei, T., Yonesaki, Y., Kinomura, N., Sato, T., 2012. J. Phys.: Conf. Ser. 339, 012004.
Dutta, S., Mandal, N., Bandyopadhyay, D., 2016. Biosens. Bioelectron. 78, 447–453.
Francis, P.T., Palmer, A.M., Snape, M., Wilcock, G.K., 1999. J. Neurol. Neurosurg. Psychiatry 66, 137–147.
Guerrieri, A., Lattanzio, V., Palmisano, F., Zambonin, P.G., 2006. Biosens. Bioelectron. 21, 1710–1718.
Hummers, W.S., Offeman, R.E., 1958. J. Am. Chem. Soc. 80, 1339.
Jun, Y., Chenghua, S.F., Tan, X.H., Ping, C.S., Qu, S.Z., Jingkun, X., 2010. Sol. Energy Mater. Sol. Cells 94, 390–394.
Lee, S.-R., Lee, H.-E., Kang, Y.O., Hwang, W.-S., Choi, S.-H., 2014. Adv. Mater. Sci. Eng., 1–12.
Liu, Y., Yu, D., Zeng, C., Miao, Z., Dai, L., 2010. Langmuir 26, 6158–6160.
Lopez, M.S., Perez, J.P.H., Lopez-Cabarcos, E., Lopez-Ruiz, B., 2007. Electroanalysis 19, 370–378.
Ming, L., Liling, T., Tongyi, L., Meeling, C., Jia, Z., Hui, R.T., Shiqiang, B., 2014. J. Phys. Chem. C 118, 10903–10910.
Mkhoyan, K.A., Contryman, A.W., Silcox, J., Stewart, D.A., Eda, G., Mattevi, C., Miller, S., Chhowalla, M., 2009. Nano Lett. 9, 1058–1063.
Pundir, C.S., Chauhan, N., Rajneesh, Manjeet, Ravi, 2011. Sens. Actuators B Chem. 155, 796–803.
Pundir, S., Chauhan, N., Narang, J., Pundir, C.S., 2012. Anal. Biochem. 427, 26–32.
Ren, X., Tang, F., Liao, R., Zhang, L., 2009. Electrochim. Acta 54, 7248–7253.
Rizzo, S., Rivière, C., Piazzi, L., Bisi, A., Gobbi, S., Bartolini, M., Andrisano, V., Morroni, F., Tarozzi, A., Monti, J.P., Rampa, A., 2008. J. Med. Chem. 51, 2883–2886.
Romllon, R., Mlonetto, N., Marty, J.L., 1992. Anal. Chim. Acta 268, 347–350.
Sajjadi, S., Ghourchian, H., Rahimi, P., 2011. Electrochim. Acta 56, 9542–9548.
Sen, S., Gülce, A., Gülce, H., 2004. Biosens. Bioelectron. 19, 1261–1268.
Shao, Y.Y., Wang, J., Wu, H., Liu, J., Aksay, I.A., Lin, Y.H., 2010. Electroanalysis 22, 1027–1036.
Shimomura, T., Itoh, T., Sumiya, T., Mizukami, F., Ono, M., 2009. Enzym. Micro Tech.

45, 443–448.
Sriprachuabwong, C., Karuwan, C., Wisitsorrat, A., Phokharatkul, D., Lomas, T., Sritongkham, P., Tuantranont, A., 2012. J. Mater. Chem. 22, 5478–5485.
Wang, H., Hao, Q., Yang, X., Lu, L., Wang, X., 2010. ACS Appl. Mater. Interfaces 2, 821–828.
Wang, W., Guiyun, X., Xinyan, T.C., Ge, S., Xiliang, L., 2014. Biosens. Bioelectron. 58, 153–156.
Xiaoliang, Y., Yongling, D., Kaiyue, D., Daban, L., Chunming, W., Shi, X., 2014. Sens. Actuators B Chem. 203, 271–281.
Xue, W., Cui, T., 2008. Sens. Actuators B Chem. 134, 981–987.
Yajie, Y., Shibin, L., Wenyao, Y., Wentao, Y., Jianhua, X., Yadong, J., 2014. ACS Appl. Mater. Interfaces 6 (16), 13807–13814.
Yang, M., Yang, Y., Yang, Y., Shen, G., Yu, R., 2005. Anal. Chim. Acta 530, 205–211.
Zhang, J., Zhang, F., Yang, H., Huang, X., Liu, H., Zhang, J., Guo, S., 2010. Langmuir 26, 6083–6085.

Please cite this article as: Chauhan, N., et al., Biosensors and Bioelectronics (2016), http://dx.doi.org/10.1016/j.bios.2016.06.047